ELSEVIER

Ecological Modelling 124 (1999) 99–119

ECOLOGICAL MODELLING

www.elsevier.com/locate/ecolmodel

Daily canopy photosynthesis model through temporal and spatial scaling for remote sensing applications

J.M. Chen [a,*], J. Liu [a], J. Cihlar [a], M.L. Goulden [b]

[a] *Canada Centre for Remote Sensing, 588 Booth Street, Ottawa, Ont., Canada K1A 0Y7*
[b] *Department of Earth System Science, University of California, Irvine, CA 92717-3100, USA*

Received 16 June 1998; received in revised form 7 June 1999; accepted 10 June 1999

Abstract

Because Farquhar's photosynthesis model is only directly applicable to individual leaves instantaneously, considerable skill is needed to use this model for regional plant growth and carbon budget estimations. In many published models, Farquhar's equations were applied directly to plant canopies by assuming a plant canopy to function like a big-leaf. This big-leaf approximation is found to be acceptable for estimating seasonal trends of canopy photosynthesis but inadequate for simulating its day-to-day variations, when compared with eddy-covariance and gas-exchange chamber measurements from two boreal forests. The daily variation is greatly dampened in big-leaf simulations because the original leaf-level model is partially modified through replacing stomatal conductance with canopy conductance. Alternative approaches such as separating the canopy into sunlit and shaded leaf groups or stratifying the canopy into multiple layers can avoid the problem. Because of non-linear response of leaf photosynthesis to meteorological variables (radiation, temperature and humidity), considerable errors exist in photosynthesis calculation at daily steps without considering the diurnal variability of the variables. To avoid these non-linear effects, we have developed an analytical solution to a simplified daily integral of Farquhar's model by considering the general diurnal patterns of meteorological variables. This daily model not only captures the main effects of diurnal variations on photosynthesis but is also computationally efficient for large area applications. Its application is then not restricted by availability of sub-daily meteorological data. This scheme has been tested using measured CO_2 data from the Boreal Ecosystem–Atmosphere Study (BOREAS), which took place in Manitoba and Saskatchewan in 1994 and 1996.

Keywords: Farquhar model; Canopy photosynthesis; Sunlit/shaded leaves; CO_2 flux; Net primary productivity; BOREAS; Remote sensing application

1. Introduction

In recent years, modeling net primary productivity (NPP) of terrestrial ecosystems has been a subject of increasing interest because of the importance of terrestrial carbon cycle in global car-

* Corresponding author. Tel.: +1-613-9471266; fax: +1-613-9471406.
E-mail address: jing.chen@ccrs.nrcan.gc.ca (J.M. Chen)

0304-3800/99/$ - see front matter
PII: S0304-3800(99)00156-8

bon budget and climate change. Several process models of NPP have been developed for this purpose and applied to global landmass at spatial resolution of 0.5–5° (Melillo et al., 1993; Bonan, 1995; Woodward et al., 1995; Foley et al., 1996; Sellers et al., 1996). Some models (Bonan, 1995; Denning et al., 1996; Foley et al., 1996) are run at small time steps (minute to hours) and coarse spatial resolutions (2–5°) in conjunction with General Circulation Models (GCM). Some process models are run at moderate spatial resolutions (1 km and larger) but at large time steps from daily to monthly, with use of remote sensing data (Running et al., 1989; Liu et al., 1997) or other data (Woodward et al., 1995). For regional and global applications, modelers usually face the choice between temporal and spatial resolutions, and modeling methodologies can be very different for these two choices. Hourly and sub-hourly models usually treat each time step calculation as instantaneous and no temporal integration is made, but such models suffer from the need for, and inaccuracy of, spatial scaling. Heterogeneity of the earth's surface makes such scaling a considerable challenge (Pielke et al., 1991; Hall et al., 1992; Bonan et al., 1993; Wood and Lakshmi, 1993). When run independent of GCMs, the high-temporal resolution models are limited by data availability. With the use of daily or monthly models, the spatial resolution can be improved and errors due to spatial scaling can be reduced. However, many detailed canopy processes cannot be simulated at large time steps, and models have to become more empirical as the modeling time step increases.

Daily models are appropriate for medium-high spatial resolution remote sensing applications because of their moderate demand on computation and input data. Since the diurnal variations of solar radiation and temperature and the associated canopy processes generally follow predictable patterns, daily models, when correctly parameterized, can capture most of the day-to-day variability in the plant canopies. Several daily models have been developed to consider the non-linear effect of diurnal variation in incident solar radiation on photosynthesis. Hanson (1991) found an analytical solution to the daily integral of an empirical photosynthesis model as a rectangular hyperbola function of radiation. Haxeltine and Prentice (1996) developed a daily model using a non-rectangular hyperbola function to describe the effect of radiation on photosynthesis. Sands (1995) adjusted a light use efficiency model according to the diurnal radiation variation patterns. These models as well as others with specific consideration of methods of photosynthesis calculation after daily and monthly input data aggregations (Trost, 1990; Aber et al., 1996; Liu, 1996) suggest the importance of considering the variability of meteorological conditions within a computation time step. However, some existing daily models using Farquhar's formulation (Farquhar et al., 1980), such as the BIOME-BGC (Hunt and Running, 1992; Kimball et al., 1997), have not explicitly incorporated the diurnal variation patterns in the calculations. When we applied these daily models to reliable data sets obtained from Boreal Ecosystem–Atmosphere Study (BOREAS), we found them to be incapable of simulating the day-to-day variations, and daily outputs are not reliable even though the annual totals can be brought to agreement with experimental data through parameter adjustments. To improve the daily modeling methodology without incurring much additional computation, we developed a new daily model through analytical spatial and temporal integration of canopy photosynthesis processes under some assumptions. The purpose of this paper is to present this new daily model of net primary productivity.

Because the Farquhar model was initially developed and validated for individual leaves, considerable skill is needed in using it for a plant canopy. Although the big-leaf approximation has been shown to be successful for modeling evapotranspiration for plant canopies (Monteith and Unsworth, 1990), the same approximation may be erroneous for photosynthesis because of the additional leaf internal control on carbon assimilation. For example, when stomatal conductance is replaced by canopy conductance (usually stomatal

conductance times leaf area index) in the big-leaf model constructed using Farquhar's formulation, the calculated results will be very different from the sum of photosynthesis of individual layers of leaves calculated using the same formulation because the internal control of leaves causes nonlinear response of leaf photosynthesis to stomatal conductance. From this perspective, the big-leaf methodology used by BIOME-BGC needs to be further examined using experimental data. Many studies have demonstrated successful use of Farquhar's model at the canopy level using other approaches, such as vertical integration against radiation gradient (Baldocchi, 1993; Bonan, 1995) and separation of a canopy into sunlit and shaded portions (Kim and Verma, 1991; Norman, 1993; Foley et al., 1996; De Pury and Farquhar, 1997; Wang and Leuning, 1998). We adopted and modified the latter approach because of its simplicity and ability to capture the major variability within the canopy. However, the effective use of Farquhar's model at the daily time step has not been demonstrated in previous studies. The objectives of this paper are: (1) to derive an analytical solution to a simplified temporal integral of Farquhar's photosynthesis model; (2) to validate the model using experimental results from two major boreal tree species; and (3) to show the advantages of this model over previous daily models and the limitations due to assumptions made in the derivation of the integrated daily model.

2. Daily model description

NPP is an important component of the terrestrial carbon cycle. It is defined as the new carbon stored in living plants per unit time (usually annually) per unit surface area. Using the same definition as previous studies (see review by Melillo et al., 1996), NPP is the difference between the gross primary productivity (GPP) and plant autotrophic respiration (R). The emphasis of this study is placed on the modeling of the NPP at daily step, although all other autotrophic respiration components are also calculated with the most recently published results for the purpose of model validation using experimental data.

2.1. Instantaneous leaf-level gross photosynthesis

Among models of photosynthetic CO_2 assimilation by plant leaves, the mechanistic model proposed by Farquhar et al. (1980) has been widely used. The model describes the leaf gross photosynthesis rate at an instant of time for C_3 plants as the minimum of:

$$W_c = V_m \frac{C_i - \Gamma}{C_i + K} \tag{1a}$$

and

$$W_j = J \frac{C_i - \Gamma}{4.5C_i + 10.5\Gamma} \tag{1b}$$

where W_c and W_j are Rubisco-limited and light-limited gross photosynthesis rates in μmol m^{-2} s^{-1}, respectively. V_m is the maximum carboxylation rate in μmol m^{-2} s^{-1}; J is the electron transport rate in μmol m^{-2} s^{-1}; C_i is the intercellular CO_2 concentration; Γ is the CO_2 compensation point without dark respiration; K is a function of enzyme kinetics. The dimension for C_i, Γ, and K can be either in Pa or in ppmv (parts per million by volume). Pa is used in this paper. Both Γ and K are temperature-dependent parameters. Γ, derived from Collatz et al. (1991), Sellers et al. (1992), can be expressed as:

$$\Gamma = 1.92*10^{-4}O_2 1.75^{(T-25)/10} \tag{2}$$

where O_2 is the oxygen concentration in the atmosphere, being 21,000 Pa assuming that the atmospheric pressure is 100,000 Pa and O_2 occupies 21% of the air by volume. T is the air temperature in °C. K is given by:

$$K = K_c(1 + O_2/K_o) \tag{3}$$

where K_c and K_o are Michaelis–Menten constants for CO_2 and O_2, respectively in Pa. $K_c = 30*2.1^{(T-25)/10}$, and $K_o = 30{,}000*1.2^{(T-25)/10}$ (Collatz et al., 1991). V_m can be expressed as a function of temperature (Collatz et al., 1991) or a function of both temperature and leaf nitrogen content (Bonan, 1995):

$$V_m = V_{m25}\, 2.4^{(T-25)/10} f(T) f(N) \tag{4}$$

where V_{m25} is V_m at 25°C, and is a variable depending on vegetation type; $f(T)$ and $f(N)$ are

temperature and nitrogen limitation terms defined as:

$$f(T) = (1 + \exp((-220{,}000 + 710(T + 273)) / (R_{gas}(T + 273)))))^{-1} \quad (5a)$$

$$f(N) = N/N_m \quad (5b)$$

where N is the leaf nitrogen content, and N_m is the maximum nitrogen content. J is dependent on photosynthetic photon flux density (PPFD) absorbed by the leaf (Farquhar and von Caemmerer, 1982) and is given by:

$$J = J_{max}\mathrm{PPFD}/(\mathrm{PPFD} + 2.1{*}J_{max}) \quad (6)$$

where J_{max} is the light-saturated rate of electron transport in the photosynthetic carbon reduction cycle in leaf cells. According to Wullschleger (1993), it is related to the Rubisco activity by:

$$J_{max} = 29.1 + 1.64{*}V_{m.} \quad (7)$$

To get net CO_2 assimilation rate (A), daytime leaf dark respiration (R_d) is subtracted from Eqs. (1a) and (1b):

$$A = \min(W_c, W_j) - R_d \quad (8)$$

According to Collatz et al. (1991),

$$R_d = 0.015V_m \quad (9)$$

2.2. Leaf-level daily integration of photosynthesis rate

The above instantaneous photosynthesis model at leaf level defines the photosynthetic processes of individual leaves with known light illuminance at an instant of time. Strictly, the productivity from a single leaf needs to be calculated continuously for the course of a day to obtain the daily total. Such a calculation for a large area is impossible from both viewpoints of meteorological data availability and computational demand. For regional and global applications, this original instantaneous model has been used to represent the mean photosynthesis rate for periods of different lengths from day to month (Woodward et al., 1995; Kimball et al., 1997). In these previous applications, reasonable values for photosynthesis can be obtained through appropriate parameter adjustments while ignoring the variability within one time step. In order to avoid the excessive computational demand of diurnal calculation through numerical integration and yet to consider the effects of diurnal variation patterns of meteorological variables on photosynthesis, we developed an analytical solution to the simplified temporal integral of Farquhar's model for calculations at daily time steps.

The net photosynthesis rate can also be described in the form (Leuning, 1990; Sellers et al., 1996):

$$A = (C_a - C_i)g \quad (10)$$

where C_a is CO_2 concentration in the atmosphere; g is the conductance to CO_2 through the pathway from the atmosphere outside of leaf boundary layer in μmol m^{-2} s^1 Pa^{-1} to the intercellular space, given by:

$$g \approx 10^6{*}g_s/(R_{gas}{*}(T + 273)) \quad (11)$$

where g_s is stomatal conductance; R_{gas} is the molar gas constant, being 8.3143 m^3 Pa mol^{-1} K^{-1}. After (i) substituting C_i in Eqs. (1a) and (1b) with Eq. (10), (ii) combining the results with Eq. (8), and (iii) choosing the solution of the quadratic equations with the smaller roots (Leuning, 1990), we obtain:

$$A_c = \frac{1}{2}((C_a + K)g + V_m - R_d - \sqrt{((C_a + K)g + V_m - R_d)^2 - 4(V_m(C_a - \Gamma) - (C_a + K)R_d)g)} \quad (12a)$$

$$A_j = \frac{1}{2}((C_a + 2.3\Gamma)g + 0.2J - R_d - \sqrt{((C_a + 2.3\Gamma)g + 0.2J - R_d)^2 - 4(0.2J(C_a - \Gamma) - (C_a + 2.3\Gamma)R_d)g)} \quad (12b)$$

where A_c and A_j correspond to W_c and W_j, respectively, after a small reduction for dark respiration (see Eq. (8)).

The diurnal variation in plant photosynthesis is caused by several meteorological variables including (1) incident solar irradiance which determines stomatal conductance and J in the photosynthesis model; (2) air temperature which affects V_m, Γ, and K; and (3) air humidity which influences stomatal conductance and hence C_i. Complete temporal integration of Eqs. (12a) and (12b) re-

quires consideration of the temporal patterns of all three variables, but no analytical solutions to this complete daily integral are possible. Through our numerical experiments with the daily integral, we found that the diurnal variation in photosynthesis is mostly caused by the diurnal variation in stomatal conductance as the synthetic variable of the solar irradiance and vapor pressure deficit under given soil moisture conditions. The effect of the air temperature variation is secondary and generally occurs in a similar pattern to solar radiation. This is agreeable since solar radiation is the driving force for diurnal changes in other meteorological variables. Incident solar irradiance, air temperature and humidity at a given location are usually highly correlated. Our temporal scaling approach is therefore focused on the diurnal integration of changes caused by stomatal conductance. For the calculation of diurnal course of stomatal conductance, we made the following assumptions.

1. The daily course of solar radiation follows a cosine function of solar zenith angle with a peak at solar noon. That is:

$$S_g = S_{g,n}\cos\left(\frac{\theta-\theta_n}{\pi/2-\theta_n}\frac{\pi}{2}\right) \tag{13}$$

where S_g is the instantaneous global solar radiation; $S_{g,n}$ is the global solar radiation at noon; θ is the solar zenith angle; θ_n is the solar zenith angle at noon. This equation is applied to sunlit leaf calculations on all weather conditions. A cloudy day follows the same pattern as a clear day but with smaller magnitudes.

2. Solar radiation variation determines the diurnal pattern of stomatal conductance. Since air humidity has a similar diurnal pattern, the first order effect of humidity is automatically brought into account in this way. However, considerable errors can still remain after considering these variations because under water-stressed conditions, plants usually exhibit mid-day depression in photosynthesis as a result of low leaf water potential. Such effects causing irregular diurnal patterns are difficult to be considered at daily step calculations, but the water potential effect will enter into the calculation through making the mid-day stomatal conductance dependent on the daily mean water potential.

3. V_m, K and J in Eqs. (12a) and (12b) change approximately linearly with environmental factors during the day so that daily mean values for them can be used. We realize that V_m and K are non-linear functions of temperature. However, during the active photosynthesis period in the day, the temperature generally vary within a small range (5–10°C), and the departure from the linearity is small within such a small range. The sunlit and shaded leaf separation described below is the critical step towards minimizing the non-linear effect of the spatial variability of PPFD in the canopy on J, but the effect of temporal variability still remains. However, the most important effect of PPFD temporal variability on stomatal conductance is considered.

4. The ratio of sunlit to shaded leaf area is constant during a day. This ratio does vary during the day and decreases with increasing solar zenith angle. This simplification is made to avoid excessive complexity of the model. The simplification causes some suppression of diurnal variation, which is compensated by assuming the sinusoidal variations in the direct and diffuse irradiance on leaf surfaces.

Theoretically, diurnal integration of Eqs. (12a) and (12b) for daily total photosynthesis should be made with respect to time. Our attempt to obtain an analytical solution to such integration was not successful because of the complication induced by the non-linear relationship between time and stomatal conductance, which is approximately sinusoidal. We therefore found an alternative by integrating with respect to conductance (g) as follows:

$$A_c = \frac{\mu}{2(g_n-g_{min})}\int_{g_{min}}^{g_n}((C_a+K)g+V_m-R_d - \sqrt{((C_a+K)g+V_m-R_d)^2-4(V_m(C_a-\Gamma) - (C_a+K)R_d)g)}\,dg \tag{14a}$$

$$A_j = \frac{\mu}{2(g_n-g_{min})}\int_{g_{min}}^{g_n}((C_a+2.3\Gamma)g+0.2J-R_d - \sqrt{((C_a+2.3\Gamma)g+0.2J-R_d)^2-4(0.2J(C_a - \Gamma)-(C_a+2.3\Gamma)R_d)g)}\,dg \tag{14b}$$

where g_n is the conductance at noon, and g_{min} is the minimum conductance before sunrise or after sunset and is set to zero in this study. The underlying assumption of direct integration with respect to g rather than time is that g changes linearly with time in both directions from noon. Since the diurnal solar radiation variation pattern is more sinusoidal than linear, such an assumption can incur errors in the final integration. If g_n is correctly calculated from the total daily radiation and leaf water potential using the sinusoidal pattern, the linear variation would cause underestimation in the daily photosynthesis. There are two ways to remedy this: (1) to calculate g_n under the same linear assumption, (2) to make an adjustment according to the difference between these two integration schemes. The first is not a good choice because it would produce g_n which is unrealistic and cannot be compared with measurements. We choose to correct the bias by making an adjustment. The parameter μ is therefore multiplied to the integral. It can be calculated from

$$\mu = \frac{1}{0.5\pi/2}\int_0^{\pi/2} \cos\theta \, d\theta = \frac{4}{\pi} \approx 1.27 \tag{15}$$

The result is to increase the linearly-integrated value by 27%. The appropriateness of the linear integration and this adjustment lies in the fact that the relationship between A_c (or A_j) and g is essentially linear (Ball, 1988) except for very large g values (Leuning, 1990; Dang et al., 1998). With this simplification in our approach, these two equations can be analytically integrated and presented in the following form:

$$A = \frac{1.27}{2(g_n - g_{min})}\left(\frac{a^{1/2}}{2}(g_n^2 - g_{min}^2) + c^{1/2}(g_n - g_{min}^2) - \frac{2ag_n + b}{4a}d + \frac{2ag_{min} + b}{4a}e^{1/2} + \frac{b^2 - 4ac}{8a^{3/2}}\ln\frac{2ag_n + b + 2a^{1/2}d}{2ag_{min} + b + 2a^{1/2}e}\right) \tag{16}$$

where for A_c, $a = (K + C_a)^2$, $b = 2(2\Gamma + K - C_a)V_m + 2(C_a + K)R_d$ and $c = (V_m - R_d)^2$ and for A_j, $a = (2.3\Gamma + C_a)^2$, $b = 0.4(4.3\Gamma - C_a)J + 2(C_a + 2.3\Gamma)R_d$, and $c = (0.2J - R_d)^2$. For both, $d = (ag_n^2 + bg_n + c)^{1/2}$ and $e = (ag_{min}^2 + bg_{min} + c)^{1/2}$.

Eq. (16) is the final equation for calculating the daily averaged A as the minimum of A_c and A_j. It is applied to sunlit and shaded leaves separately. It is noted that: (1) no additional parameters are introduced in this daily model, and all the constants are determined by the leaf biochemical parameters in the original Farqhuar model; (2) although Eq. (16) appears to be complex, it is numerically stable, and no numerical problems have been encountered in using this equation for remote sensing applications for large areas of extreme conditions; (3) the analytical integration given by Eq. (16) is computationally efficient and avoids a daily loop using a numerical integration method.

In principle, Eq. (16) should be applied for every leaf in a canopy in order to get daily or monthly total canopy photosynthesis. In this study, we choose to stratify a canopy into sunlit and shaded leaf groups and apply this equation to these two groups separately. We prefer this to stratification by canopy layers because the greatest difference in leaf illumination in the canopy exists between sunlit and shaded leaves. The purpose of the multiple layer calculation is to consider the general decreasing trend of radiation with the increasing depth into the canopy. It is an improvement from the big-leaf model, in which the canopy is treated as one layer of leaves. However, within a layer at a given time the difference in illumination between sunlit and shaded leaves is very large and using the mean illumination value to represent the layer can result in considerable errors in modeled results. With the separation of sunlit and shaded leaf groups, the total canopy photosynthesis (A_{canopy}) can be calculated as (Norman, 1982):

$$A_{canopy} = A_{sun}LAI_{sun} + A_{shade}LAI_{shade} \tag{17}$$

where the subscripts 'sun' and 'shade' denote the sunlit and shaded components of photosynthesis and LAI. The method of Norman (1982) for calculating LAI_{sun} and LAI_{shade} is adopted in this study but modified to consider the effect of foliage clumping index (Ω) on the canopy radiation regime:

$$\mathrm{LAI_{sun}} = 2\cos\theta(1-\exp(-0.5\Omega\mathrm{LAI}/\cos\theta)) \quad (18a)$$

$$\mathrm{LAI_{shade}} = \mathrm{LAI} - \mathrm{LAI_{sun}} \quad (18b)$$

where LAI is the leaf area index, and θ is the solar zenith angle. Ω for boreal forests is ~ 0.5 for conifers and 0.7 for deciduous species, respectively (Chen, 1996a; Chen et al., 1997). The larger Ω departure from unity, the more non-random is the foliage spatial distribution. It is critically important to consider this in productivity models because foliage clumping alters the way plants interact with incident radiation. Increasing foliage clumping (decreasing Ω value) allows more radiation penetrated through the canopy without being intercepted by the foliage and therefore decreases sunlit LAI and increases shaded LAI. The clumped architecture of forest canopies makes the stratification between sunlit and shaded leaves essential because the fraction of the shaded leaves is much larger in clumped canopies than in random canopies and shaded leaves play an important role in forest productivity (Goulden et al., 1997).

2.3. Sunlit leaf irradiance and shaded leaf irradiance

Sunlit leaf irradiance and shaded leaf irradiance are important variables in Eq. (16) because of their effects on both g and J. In order to estimate them, the total solar radiation above the plant canopy (S_g) is partitioned using an empirical formula of Erbs et al. (1982), which was modified and validated by Black et al. (1991) for northern environment. The fraction of diffuse radiation in the total is determined by:

$$\frac{S_{\mathrm{dif}}}{S_g} = \begin{cases} 0.943 + 0.734R - 4.9R^2 + 1.796R^3 + 2.058R^4 \\ \qquad R < 0.8 \\ 0.13 \quad R > 0.8 \end{cases} \quad (19)$$

where S_g is the global solar radiation in W m^{-2}. R is a ratio equal to $S_g/(S_o \cos\theta)$ where S_o is the solar constant ($=1367$ W m^{-2}). The direct radiation fraction above the canopy (S_{dir}) is the remainder of the diffuse fraction.

With S_{dif}, and therefore S_{dir} determined from Eq. (19), the sunlit leaf irradiance (S_{sun}) is calculated as (Norman, 1982):

$$S_{\mathrm{sun}} = S_{\mathrm{dir}}\cos\alpha/\cos\theta + S_{\mathrm{shade}} \quad (20)$$

where α is mean leaf-sun angle. $\alpha = 60°$ for a canopy with spherical leaf angle distribution, which is found to be also a good approximation for boreal canopy in θ range from 30 to 60° (Chen, 1996b). Because S_{dir} is proportional to $\cos\theta$, S_{sun} changes little in a day. With the consideration of foliage clumping effect, a different method for estimating the mean shaded leaf irradiance (S_{shade}) is developed based on radiative transfer physics. It is summarized as follows:

$$S_{\mathrm{shade}} = (S_{\mathrm{dif}} - S_{dif,under})/\mathrm{LAI} + C \quad (21)$$

where $S_{\mathrm{dif,under}}$ is diffuse radiation under the plant canopy; and C arises from multiple scattering of direct radiation (Norman, 1982):

$$C = 0.07\Omega S_{\mathrm{dir}}(1.1 - 0.1\mathrm{LAI})\exp(-\cos\theta) \quad (22)$$

Eq. (21) states that diffuse irradiance on shaded leaves originates from two sources: sky irradiance and multiple scattering of the incident radiation within the canopy. The first term in Eq. (21) makes the average of the total intercepted diffuse radiation from the sky for the total LAI involved (sunlit leaves also contribute to the interception). The diffuse radiation reaching to the forest floor is calculated using the simple equation with the consideration of the clumping effect (Ω):

$$S_{\mathrm{dif,under}} = S_{\mathrm{dif}}\exp(-0.5\Omega\mathrm{LAI}/\cos\overline{\theta}) \quad (23)$$

where $\overline{\theta}$ is a representative zenith angle for diffuse radiation transmission and slightly dependent on leaf area index:

$$\cos\overline{\theta} = 0.537 + 0.025\mathrm{LAI} \quad (24)$$

This is a simple but an effective way to calculate the transmitted diffuse radiation. It avoids the integration of the sky irradiance for the hemisphere by using a representative transmission zenith angle $\overline{\theta}$, which is obtained through a numerical experiment with the complete integration. Under the assumption of isotropic sky radiance distribution, it is near a constant of 57.5° but also a weak function of LAI. This angle is larger than the mean of 45° because the hemisphere is more heavily weighted against the lower hemisphere in the inte-

gration. The dependence on LAI is found because it modifies slightly the weight distribution.

2.4. Stomatal conductance

Plants respond to their environment through stomatal movement that can be quantified in terms of stomatal conductance. To simulate this response, one approach is to reduce a species-dependent maximum by the environmental conditions departed from the optimum (Jarvis and Morison, 1981; Running and Coughlan, 1988). The environmental factors usually include photosynthetic photon flux density (PPFD), temperature (T), vapor pressure deficit (VPD), and others, i.e.

$$g_s = \max(g_{\max} * f(\text{PPFD}) * f(T) * f(\text{VPD}),\ g_{\min}) \tag{25}$$

where the environmental functions are scalars between 0 and 1 which are formed in the same way as in BIOME-BGC. These functions are expressed as:

$$f(\text{PPFD}) = \text{PPFD} * \text{PPFD}_{\text{coef}} / (1 + \text{PPFD} * \text{PPFD}_{\text{coef}}) \tag{26a}$$

$$f(T) = \begin{cases} \ln(T)/\ln(T_{\text{opt}}) & T < T_{\text{opt}} \\ \cos\left(\frac{\pi}{2}(T - T_{\text{opt}})/(T_{\text{range}} - T_{\text{opt}})\right) & T > T_{\text{opt}} \\ 0 & T < 1 \end{cases} \tag{26b}$$

$$f(\text{VPD}) = \begin{cases} 1 & \text{VPD} < \text{VPD}_{\text{open}} \\ (\text{VPD}_{\text{close}} - \text{VPD})/(\text{VPD}_{\text{close}} - \text{VPD}_{\text{open}}) & \text{VPD}_{\text{open}} < \text{VPD} < \text{VPD}_{\text{close}} \\ 0 & \text{VPD} > \text{VPD}_{\text{close}} \end{cases} \tag{26c}$$

The meaning of the symbols in these equations and their values and units are found in Table 1.

To determine PPFD at noon, the solar zenith angle at noon is first calculated from the latitude of the location (φ) and the day of year (D) (Oke, 1990):

$$\cos\theta_{\text{n}} = \sin(-23.4\cos(360(D+10)/365))\sin\varphi + \cos(-23.4\cos(360(D+10)/365))\cos\varphi \tag{27}$$

The arguments in the trigonometry functions in Eq. (27) are in degrees. According to Eq. (13),

$$\frac{S_{\text{g, day}}}{\text{Daylength}} = \frac{1}{\frac{\pi}{2} - \theta_{\text{n}}} \int_{\theta_{\text{n}}}^{2/\pi} S_{\text{g,n}} \cos\left(\frac{\theta - \theta_{\text{n}}}{\pi/2 - \theta_{\text{n}}}\frac{\pi}{2}\right) \text{d}\theta = (2/\pi) S_{\text{g,n}} \tag{28}$$

where $S_{\text{q,day}}$ is the daily total solar radiation in J day^{-1} m^{-2}. Therefore, with the PAR-energy ratio of 4.55 μmol/J and the visible shortwave radiation fraction of 0.5, PPFD at noon (in μmol m^{-2} s^{-1}) is:

$$\text{PPFD}_{\text{n}} = 1.1\pi(S_{\text{g, day}}/\text{Daylength}) \tag{29}$$

2.5. Daily autotrophic respiration

Conventionally, autotrophic respiration (R_{a}) is separated into maintenance respiration (R_{m}) and growth respiration (R_{g}) (Running and Coughlan, 1988; Ryan, 1990, 1991):

$$R_{\text{a}} = R_{\text{m}} + R_{\text{g}} = \sum_i (R_{\text{m},i} + R_{\text{g},i}) \tag{30}$$

where i is an index for different plant components, (1 for leaf, 2 for stem, and 3 for root). Maintenance respiration is temperature-dependent:

$$R_{\text{m},i} = M_i r_{\text{m},i} Q_{10}^{(T - T_{\text{b}})/10} \tag{31}$$

where M_i is the biomass (sapwood for stems) of plant component i; $r_{\text{m},i}$ is maintenance respiration coefficient for component i, or the respiration rate at the base temperature; Q_{10} is the temperature sensitivity factor, and T_{b} is the base temperature. Growth respiration is generally considered to be independent of temperature and is proportional to GPP:

$$R_{\text{g},i} = r_{\text{g},i} r_{\text{a},i} \text{GPP} \tag{32}$$

where $r_{\text{g},i}$ is a growth respiration coefficient for plant component i; and $r_{\text{a},i}$ is the carbon allocation fraction for plant component i.

3. Experimental data for model validation

An old black spruce site located at 55.879° N and 98.484° W in Manitoba, Canada, is chosen as the major site to validate the daily model. This site was one of tower measurement sites during the BOREAS in 1994 (Sellers et al., 1997). Black spruce (*Picea mariana*) is the dominant species in the BOREAS study region. The overstory at the site was dominated with dense, 10 m tall, 75-year-old trees in upland areas, and sparse, 1 to 6-m tall, 90-year-old trees in lowland areas. The understory was composed of 45% feather moss (*Pleurozium schreberi*), 45% Sphagnum moss (*Sphagnum fuscum*), and 10% fen within 500 m of the tower. The site was level, and consisted of poorly drained silt and clay.

In 1996, simultaneous CO_2 flux measurements were made above and below the canopy. The above-canopy measurements were made using an eddy-covariance method, and the below-canopy was made using closed clear chambers on the forest floor including the understory grass and moss. Two chambers were used for feather moss (chambers 2 and 3 referred by Goulden and Crill, 1997), and three for sphagnum moss (chambers 8, 9, 10). The chamber measurements were made automatically at 3-h intervals. Daily total fluxes for the stand were obtained by giving 50% weight to the average of chambers 2 and 3 for feather

Table 1
The parameters, their descriptions, and values at the old black spruce site for NPP calculation

Symbol	Unit	Description	Value	Reference
General				
LAI	m^2/m^2	Leaf area index	4	Chen et al. (1997)
φ	° N	Latitude	55.879	Goulden et al. (1997)
Photosynthesis				
g_{max}	mm s^{-1}	Maximum stomatal conductance	1.6	Dang et al. (1997), Running and Coughlan (1988)
g_{min}	mm s^{-1}	Minimum stomatal conductance	0.0	This study
N_{leaf}	%	Leaf nitrogen content	1.2	Based on Kimball et al. (1997)
N_m	%	Maximum leaf nitrogen content	1.5	Bonan (1995)
$V_{m,25}$	μmol m^{-2} s^{-1}	Maximum carboxylation rate at 25°C	33	Bonan (1995), Dang et al. (1998)
$PPFD_{coef}$	μmol m^{-2} s^{-1}	Coefficient in a relationship between g_s and PPFD (Eq. (26a))	0.01	Kimball et al. (1997)
T_{opt}	°C	Optimal temperature	25	Kimball et al. (1997)
T_{range}	°C	Maximum temperature range	40	Kimball et al. (1997)
VPD_{open}	kPa	Vapour pressure deficit at stomatal opening	0.2	Dang et al. (1997)
VPD_{close}	kPa	Vapour pressure deficit at stomatal closure	2	Dang et al. (1997)
Respiration				
Q_{10}	–	Temperature sensitivity factor	2.3	Kimball et al. (1997)
M_{leaf}	kg C m^{-2}	Biomass of leaf	0.4	Gower et al. (1977)
M_{stem}	kg C m^{-2}	Sapwood carbon of stem	0.28	Kimball et al. (1997)
M_{root}	kg C m^{-2}	Biomass of root	1.4	Steele et al. (1997)
$r_{m,leaf}$	day^{-1}	Leaf maintenance respiration coefficient	0.002 at 20°C	Kimball et al. (1997)
$r_{m,stem}$	g g^{-1}day	Stem maintenance respiration coefficient	0.001 at 20°C	Kimball et al. (1997)
$r_{m,rootc}$	g g^{-1}day	Coarse root maintenance respiration coefficient	0.001 at 20°C	Kimball et al. (1997)
$r_{m,rootf}$	g g^{-1}day	Fine root maintenance respiration coefficient	0.002 at 20°C	Kimball et al. (1997)
r_g	g g^{-1}day	Overall growth respiration coefficient	0.25	Ryan (1991)
$r_{g,root}$	g g^{-1}day	Root growth respiration coefficient	0.25	Ryan (1991)
$r_{a,root}$	–	Root carbon allocation fraction	0.40	Running and Coughlan (1988)

moss, and 50% weight to the average of chambers 8, 9 and 10 for sphagnum moss. This weight distribution reflects the percentage coverage of these two moss types on the forest floor. The data were checked for quality in processing (Goulden and Crill, 1997) and good measurements from 28 May to 21 October, 1996 were used in this study. Similar above-canopy measurements in 1994 and below-canopy measurements in 1995 were described in detail by Goulden et al. (1997), Goulden and Crill (1997), respectively.

The flux measurements at these two levels can be used to differentiate between the overstory and the background (understory, moss and soil) in their role in the carbon cycle. The fluxes at the top of the canopy and from the forest floor are composed of several terms defined as follows:

$$\mathrm{FLUX_T} = P_{\mathrm{OVER}} + R_{\mathrm{OVER,ABOVE}} + R_{\mathrm{OVER,ROOT}} + P_{\mathrm{UNDER}} + R_{\mathrm{UNDER}} + R_{\mathrm{SOIL}} \quad (33)$$

$$\mathrm{FLUX_C} = R_{\mathrm{OVER,ROOT}} + P_{\mathrm{UNDER}} + R_{\mathrm{UNDER}} + R_{\mathrm{SOIL}} \quad (34)$$

where P and R denote photosynthesis and respiration fluxes, respectively. Subscripts T and C stand for tower and chamber measurements, respectively. The subscripts OVER, UNDER, SOIL indicate overstory, understory and soil, respectively. The subscripts ABOVE and ROOT are for above ground, and root of the overstory, respectively. We define downward fluxes as positive and upward fluxes as negative so that photosynthesis is always positive and respiration is always negative. Therefore, NPP of the overstory, defined as $P_{\mathrm{over}} + R_{\mathrm{over,above}} + R_{\mathrm{over,root}}$, can be then be obtained by taking the difference between Eqs. (33) and (34). The final expression becomes

$$\mathrm{NPP} = \mathrm{FLUX_T} - \mathrm{FLUX_C} + R_{\mathrm{OVER,ROOT}} \quad (35)$$

The root respiration term remains in the expression because of the transport of some fraction of carbon assimilates to roots from the overstory. Since the fluxes measured correspond to the instantaneous photosynthesis and respiration processes, NPP calculated in this way is considered to be instantaneous. Meteorological variables including solar radiation, temperature and humidity used as the model input were measured on the tower above the canopy (Goulden et al., 1997).

A deciduous forest site located at 53.629° N, 106.2° W in the BOREAS region is used to further validate the daily model. The overstory at the site was mature aspen (*Populus tremuloides*). The same principles given above are also used to obtain the overstory NPP from simultaneous eddy-covariance measurements at heights above the forest and between the overstory and understory. More details of the measurement procedures and the data set in 1994 are found in Black et al. (1996).

3.1. Parameterization for the old black spruce site

Table 1 summarizes all the parameters used for calculating photosynthesis, maintenance respiration, growth respiration and total root respiration at the old black spruce site.

3.1.1. Maximum stomatal conductance (g_{max})

The observed stomatal conductance for black spruce during BOREAS reached 0.05 mol m^{-2} s^{-1} in the field and 0.055 mol m^{-2} s^{-1} in the laboratory (Dang et al. 1997). It is $\sim$1.3–1.4 mm s^{-1}. Although the g_{max} was reduced to 1.0 mm s^{-1} in BIOME-BGC from 1.6 mm s^{-1} in the FOREST-BGC for conifer forest (Kimball et al., 1997), we consider 1.6 mm s^{-1} is more reasonable for g_{max}. It is slightly larger than the largest value found in observation because the optimum conditions seldom occurred in the field.

3.1.2. Maximum carboxylation rate at 25°C ($V_{m,25}$)

$V_{\mathrm{m,25}}$ is a very important parameter that strongly influences the magnitude of photosynthesis. Comparing the observed V_{m} values (Dang et al. 1998) with V_{m} values calculated using the methods of Bonan (1995), Kimball et al. (1997) and Sellers et al. (1992), it is found that Bonan's method and the associated $V_{\mathrm{m,25}}$ fit observations best, while the others tend to overestimate V_{m} and the photosynthetic rate.

3.1.3. Maintenance respiration coefficients

As discussed above, plant maintenance respiration is determined by: (1) biomass of plant components; (2) respiration coefficients at the base

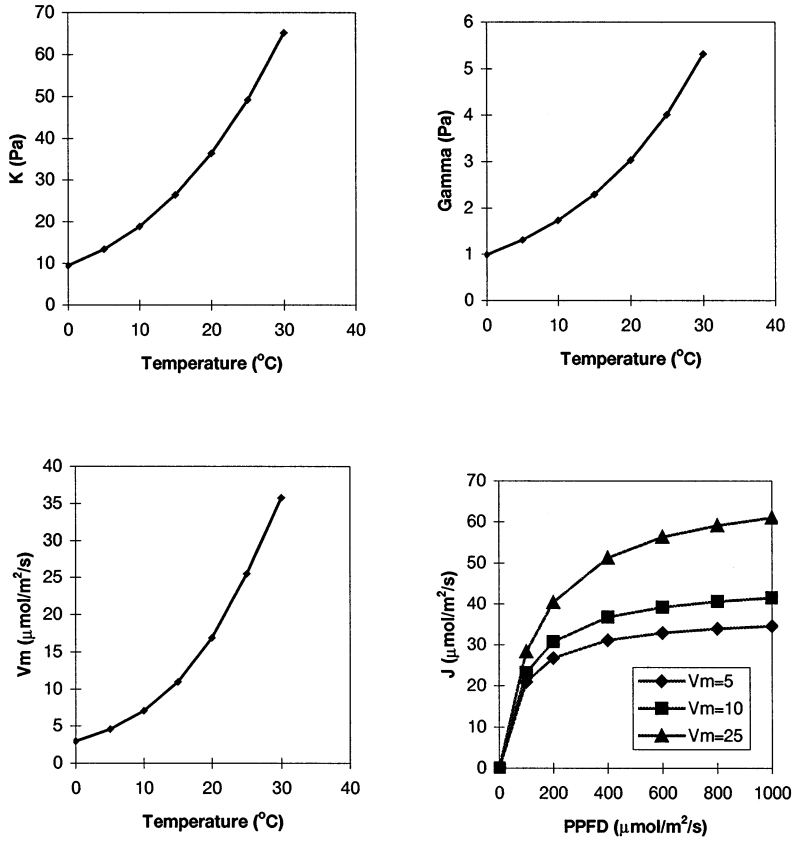

Fig. 1. Response of biochemical parameters in Farquhar's model to meteorological variables. V_m is the maximum carboxylation rate; J is the electron transport rate; gamma (Γ) is the CO_2 compensation point without dark respiration; and K is a function of enzyme kinetics.

temperature; (3) Q_{10}; and (4) base temperature. The biomass of the plant components at the site can be obtained from the literature, while determining the maintenance respiration coefficients, Q_{10} values, and the base temperature is difficult. After carefully examining previous studies (Running and Coughlan, 1988; Foley, 1994; Bonan, 1995; Ruimy et al., 1996; Kimball et al. 1997), we chose the equations and associated parameters of BIOME-BGC (Kimball et al. 1997). This is because: (1), as stated by Ruimy et al. (1996), BIOME-BGC is the only model using 'uncalibrated' coefficients; and (2) the derived autorespiration based on the coefficients agrees closely with measurements for the site (Ryan et al., 1997).

4. Results and discussion

To illustrate the importance of proper daily integration for stand-level and ecosystem-level modeling of photosynthesis, the response of several Farquhar model parameters to meteorological variables are shown in Fig. 1. The effects of temperature on the model parameters including κ, Γ and V_m are not linear, causing non-linear response to temperature over the full range. However, during daytime the temperature usually varies within a small range and a linear approximation would not incur large errors. A linear approximation justifies the use of mean daytime temperature for one step daily photosynthesis calculations. The response of J to illumination is highly non-linear. During the

daytime, plant leaves experience the full range of illumination. At a given time, leaves at different locations in the canopy can have very different illumination levels. These large temporal and spatial variations in radiation can cause large errors in daily photosynthesis calculations if ignored.

Meteorological conditions at the site during the growing season of 1996 are shown in Figs. 2 and 3. In Fig. 2, the values of the mean irradiance at noon on sunlit and shaded leaves were calculated using Eqs. (20)–(24). The day-to-day variations are caused by cloud conditions. Large day-to-day variations in air temperature and VPD are also evident in Fig. 3. The daily mean air temperature ranged from -3 to 23°C, while the daily mean VPD ranged from 0 to 16 mbar. In addition to the seasonal variation of the temperature from the end of May to the beginning of September, there were two distinct step changes in temperature at DOY ≈ 250 and DOY ≈ 270. The seasonal variation of the vapor pressure deficit follows a pattern similar to the temperature variation.

The seasonal course of daily CO_2 fluxes measured above and below the black spruce stand using eddy-covariance and chamber techniques are shown in Fig. 4. These data series are the first simultaneously paired measurements for black spruce, which allow the separation of the overstory NPP from above-canopy flux measurements on a daily basis after making an allowance for the root respiration as described in Eqs. (31) and (32). No previous models were tested with similar data sets. However, the fact that root respiration is involved causes some uncertainties in the conversion of these time series into an overstory NPP series. We therefore closely examined the magnitude of root respiration as a function of soil temperature and the root biomass. Using the available data for root biomass measured at the site and suggested coefficients (Running and Coughlan, 1988; Steele et al., 1997; Kimball et al., 1997; Ryan, 1991; Ryan et al., 1997), we obtained the best possible daily values of root respiration (Fig. 5). The total autotrophic respiration without the daytime leaf respiration is also shown for comparison. The root respiration is responsible for 60% of the total plant respiration. This ratio is in agreement with the value of 62% for the site reported by Ryan et al. (1997).

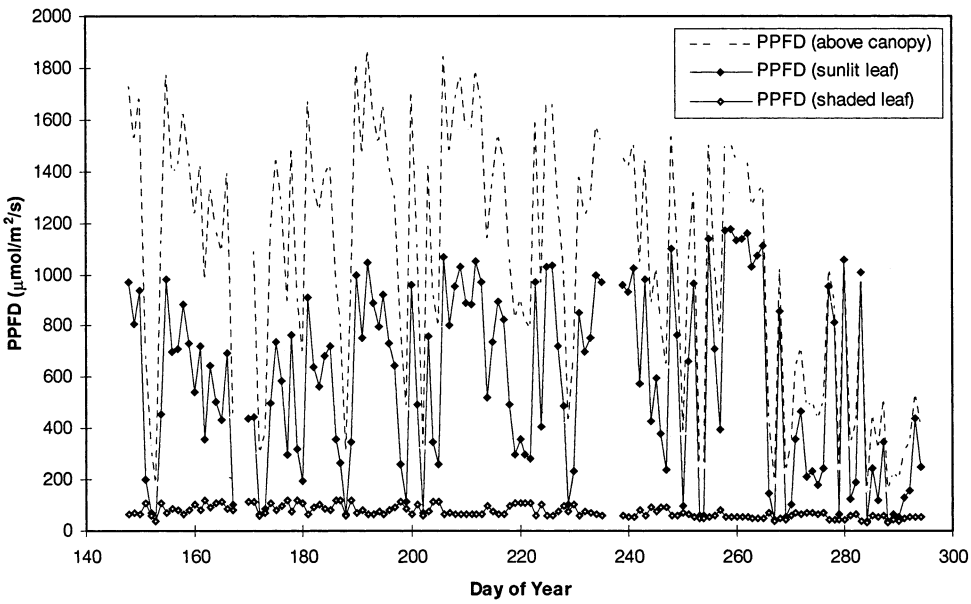

Fig. 2. Canopy photosynthetically active photon flux density (PPFD) on sunlit and shaded leaves at noon in comparison with the total PPFD at noon.

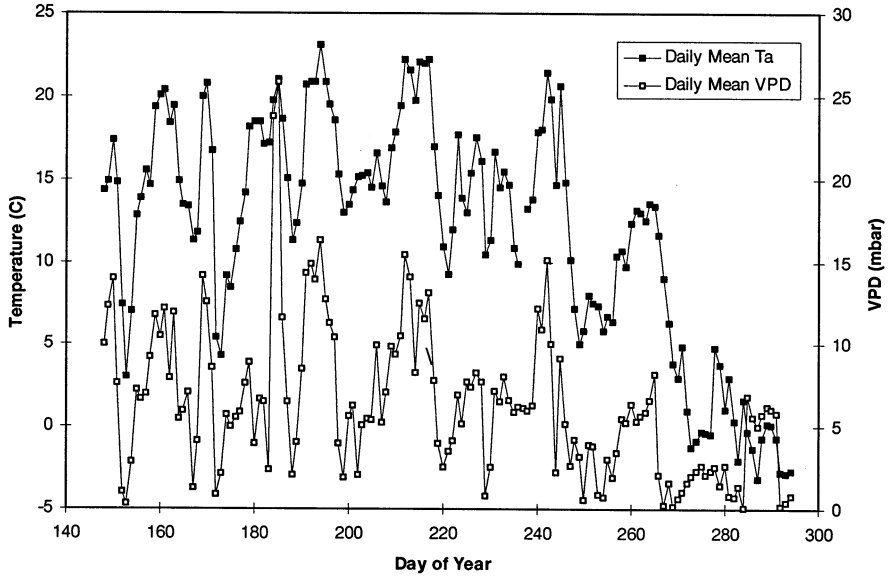

Fig. 3. Daily mean air temperature and vapor pressure deficit (VPD) measured at a micrometeorological tower above a mature black spruce stand at the height of 29 m.

Results from several models are compared with the 'measured daily NPP' values obtained from the above- and below-canopy flux measurements and root respiration estimates (Fig. 6). Three types of models were used: (1) Farquhar's model with the daily integration and sunlit–shaded leaf separation as shown in Section 2; (2) Farquhar's model with sunlit–shaded leaf separation without the daily integration; and (3) big-leaf Farqhuar's model as formulated by BIOME-BGC. The values for the model parameters of κ, Γ and V_m are found to be the most suitable for the species (Collatz et al., 1991; Bonan, 1995; Dang et al., 1998) and are the same for all three types of models. The relationship between V_m and J_{max} is also the same. The differences in the modeled results are therefore entirely due to the different mathematical manipulation of the Farquhar equations. In all these models, the soil water balance, precipitation, and evapotranspiration are considered and stomatal conductance is calculated not only from radiation but also from temperature and humidity as outlined in Eqs. (25), (26a), (26b) and (26c)–(29). Several important points are demonstrated.

(1) The big-leaf model is able to simulate the general seasonal variation pattern with approximately correct total for the season, but it is not able to mimic the day-to-day variation. Much of the day-to-day variation in photosynthesis was caused by changes in radiation regimes as well as in humidity and temperature. The effects of the changes in radiation and humidity are mostly considered through their influences on stomatal conductance and partly in the value of J. However, in the big-leaf formulation, canopy conductance as a surrogate of stomatal conductance is only a relative small part of the control of the flow of CO_2 from the free air to photosynthetic apparatus in leaf cells, and the canopy photosynthesis is not very sensitive to changes in canopy conductance. The fundamental problem with big-leaf models is that when stomatal conductance is replaced by canopy conductance, the big-leaf internal controls, as reflected by the parameters κ, Γ, V_m and J_{max}, should not remain the same. For example, if Γ is considered as the CO_2 compensation point per unit leaf area, in the big-leaf model it should become per unit ground surface area, and then the value should be increased by a factor

equal to LAI because more leaf area produces more photorespiration. By the same argument, V_m and J_{max} should also be increased accordingly. We conducted numerical experiments by increasing these parameters by a factor of LAI and found that the day-to-day variation indeed becomes much larger and follows the general pattern of measured NPP. Although this seems to be an improvement to the big-leaf formulation, it does not solve the problem because these adjustments do not have biological foundation and makes the model too highly sensitive to the input LAI value. In reality, canopy photosynthesis has diminished response to LAI increase at large LAI values. A further improvement can perhaps be made by allowing V_m and J_{max} to vary at different layers. This then will eventually turn a big-leaf model into a multiple layer model. The problem with big-leaf models can also be seen from another perspective. In a canopy, individual leaves operate in parallel, but big-leaf models conceptually force them to operate in a partial parallel mode after multiplying the stomatal conductance by LAI. When stomatal conductance is replaced by canopy conductance in Farquhar's model, the simulated leaf internal CO_2 concentration (C_i) becomes unrealistic (in some cases values very close to external concentration C_a can be produced in big-leaf simulation). This is because the harmony of the original model for individual leaves is disrupted when used in this way.

(2) The simple separation of sunlit and shaded leaves at noon results in much greater day-to-day variability compared with the big-leaf model, and the pattern of the variation is similar to that exhibited in the measured data. However, the magnitude of the modeled NPP is too large compared with measured values. The difference far exceeds the uncertainty range in the root respiration estimation. The overestimation is caused by optimizing the radiation control on photosynthesis in the process of taking the mean irradiance for the day. For example, in hourly calculations, sunlit leaves are often saturated by direct irradiance, but when the mean of the day is taken, the saturation never occurs. In this case, the radiation use efficiency is too high, resulting in the overestimation. Fig. 7 is shown in support of this argument. The modelled daily total gross primary productivity (GPP), as defined by Eqs. (1a) and

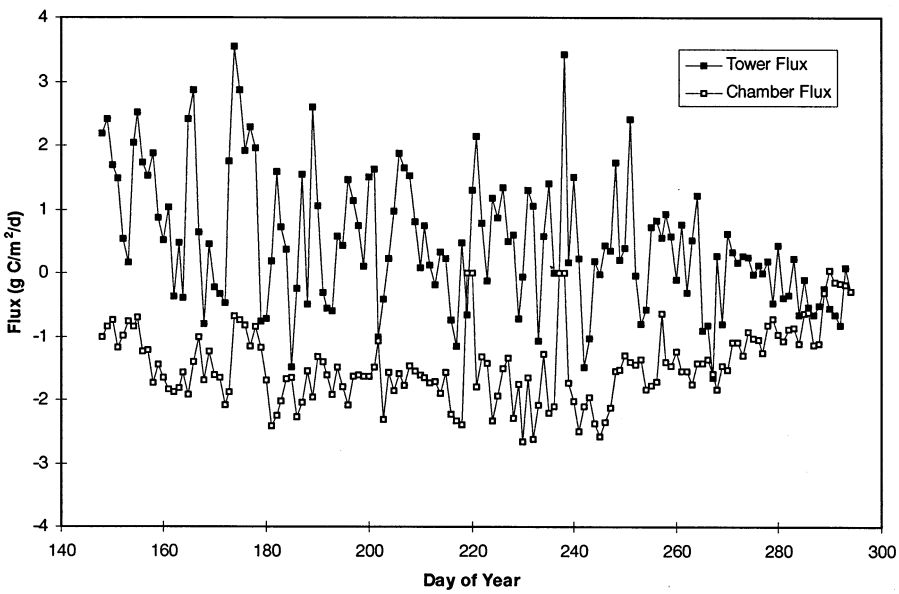

Fig. 4. Daily total CO_2 fluxes measured using an eddy-covariance technique above the canopy (29 m) and below the canopy using chambers. Note downward flux is defined as positive.

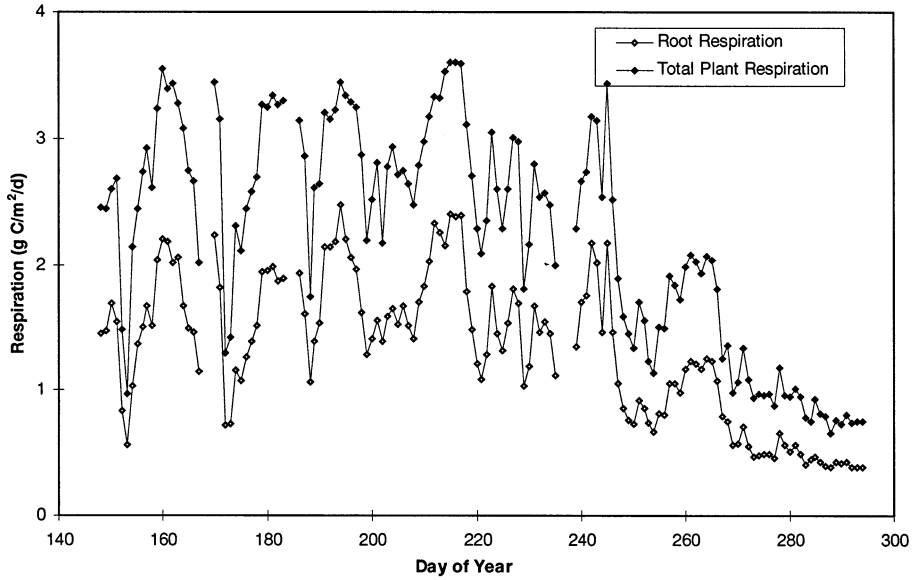

Fig. 5. Estimated daily root respiration and total plant respiration for the growing season for a mature black spruce stand.

(1b), depends strongly on the computation time step, within which the tower-measured meteorological variables (radiation, temperature and humidity) are aggregated before modelling. The modelled values increases with the increasing time step from 1/2, 2, 4 to 24 h, although the difference between 1/2 and 2 h steps is small.

(3) The integrated daily model not only has the appropriate variability but also has the right magnitude. This model not only avoids the flaws of the big-leaf model, allowing good response of predicted photosynthesis to weather conditions, but also remedies the overestimation problem of sunlit–shaded leaf model without considering the diurnal variation pattern.

Another problem with big leaf models using Farquhar's formulation is the tendency to invoke frequent temperature limitations and infrequent radiation limitations to photosynthesis. When either the incident radiation or the absorbed radiation of the big-leaf is used in the models, the estimated electronic transport rate almost always exceeds the Rubisco activity, i.e. the radiation level is higher than the minimum required by the Rubisco activity and often becomes irrelevant for canopy photosynthesis estimation. As both photosynthesis and autotrophic respiration vary with temperature in similar patterns, the NPP, as the difference between GPP and autotrophic respiration, becomes insensitive not only to radiation but also to temperature variation. The big-leaf model is therefore not able to capture productive sunny and humid days or non-productive overcast or rainy days. After sunlit and shaded leaves are separated, it is often found that sunlit leaves are controlled by temperature and shaded leaves by radiation, and therefore the sensitivity of the calculated NPP to meteorological changes is greatly improved.

Having shown shortcomings of the big-leaf formulation for canopy photosynthesis, we need to analyze the reason for the widespread success of big-leaf evapotranspiration (ET) model (Monteith and Unsworth, 1990). For transpiration, leaves in different layers also operate in parallel, but changing the formulation from the parallel to partial parallel mode in big-leaf models only incurs a small error due to the control of leaf air boundary layer resistance which is in series with stomatal resistance. If the boundary layer resistance is absent, there is no difference between parallel (multiple layers) and big-leaf (single layer)

formulations This is because the flow of water vapor remains the same whether or not it is divided into multiple channels (stomates) as long as the total conductance is the same. This may be understood by imagining the case of water flow in a pipe: the flow rate is independent of the number of divisions of the pipe into mini-pipes if the friction on the walls of the mini-pipes is ignored. The friction resembles the boundary layer resistance. Because it is usually one order of magnitude smaller than the stomatal resistance, any simple treatment of this effect does not cause considerable errors. The basic reason for the success of ET big-leaf models is that there is no leaf internal control beyond stomates on the water vapor flux, i.e. the stomatal pores are 100% wet. On the other hand, in photosynthesis, CO_2 in stomatal pores can be assimilated at very different rates depending on the rate of Rubisco activity or the electron transport. In mathematical terms, there is a large additional resistance to the CO_2 flow inside the leaf that is in series with stomatal resistance and should be adjusted accordingly when stomatal conductance is replaced by canopy conductance. From this point of view, it can be inferred that big-leaf NPP models would work well for thin canopies with LAI close to unity, but as the LAI increases the error of big-leaf models will likely to increase. If a model of this type is calibrated using measurements from a site through adjustment of parameters (such as V_{max} and Γ), it can still be inaccurate for other stands of different LAI values or under different climate regimes. In other words, the level of simplification in our modeling methodologies should be compatible with the complexity of the gas type involved in the biological processes, and it is undesirable to simplify the photosynthesis process using big-leaf models if both simplicity and generality of models are required.

The results from the big-leaf and daily-integrated models are compared with the measured daily NPP values in one-to-one plots (Fig. 8) for further analysis. The lack of response of the big-leaf model to the changes in the measured values is evident from the small slope and low R^2 value. The response is greatly increased after the sun–shade leaf separation and the daily integration,

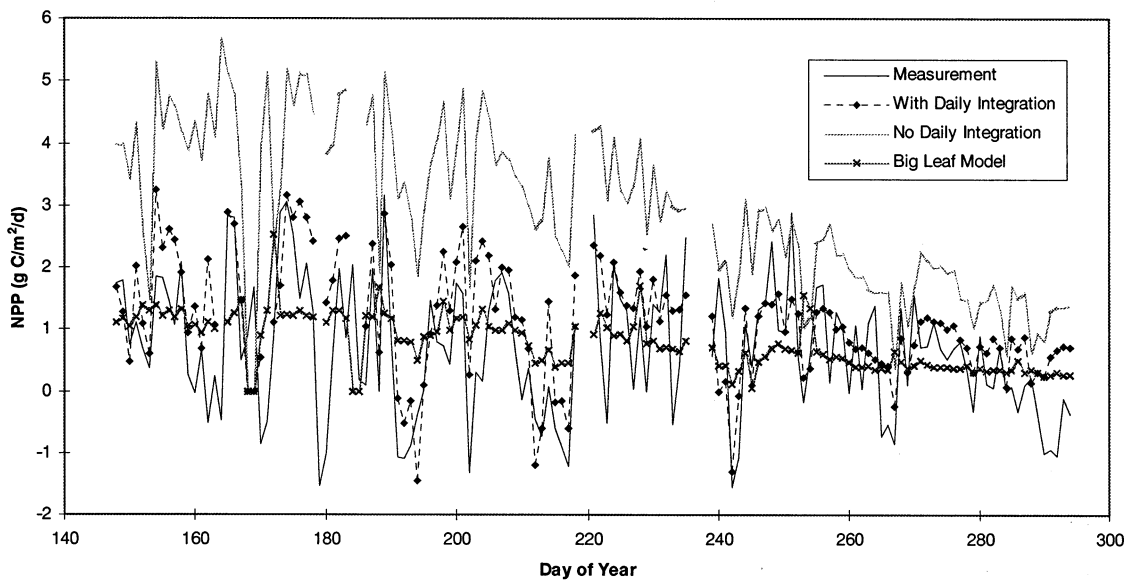

Fig. 6. Daily variations of overstory NPP obtained from tower and chamber measurements in comparison with modeled results. For all three modeling methodologies the same values were used for V_m, Γ and other coefficients in Farquhar's model. The same relationship between V_m and J_{max} was also used.

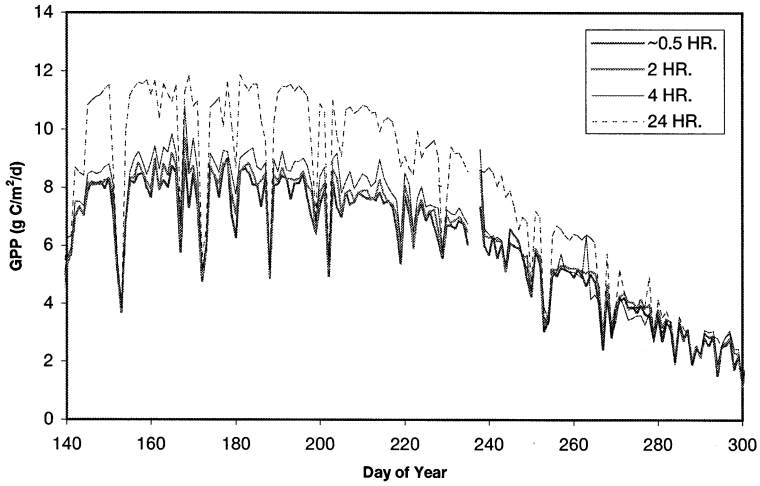

Fig. 7. The effect of pre-modelling data aggregation on daily gross primary productivity (GPP) calculations for a mature black spruce stand. The calculations are made using the sunlit–shaded leaf model without considering the variability of meteorological conditions within a time step. The data aggregation steps are 0.5, 2, 4 and 24 h.

but the deviation from the one-to-one line is still significant and the R^2 value is still low (0.46). Much of the scatter in the plot results from the uncertainties in chamber measurements because the five chambers used might have not well represented the average conditions of the stand under varying weather conditions. Some of the scatter is due to irregular sub-daily variations in weather conditions, especially on cloudy days when the diurnal radiation pattern deviates from the sinusoidal pattern assumed in the model. For the purpose of differentiating errors due to sub-daily variability from those due to measurement, daily NPP values (i.e. Y) calculated at daily steps using the sun–shade model with daily integration (Eqs. (16) and (17)) were compared with those (i.e. X) calculated at half hourly steps using a sun–shade leaf model (Eqs. (12a), (12b) and (17)). The result of the comparison is $Y = 0.94X + 0.38$, with $R^2 = 0.72$. This means that the sub-daily variability caused about half of the data scatter and the other half was due to measurement errors. The systematic difference between modeled values at these two time steps is about 22%, suggesting that there is still room for improvement in the integrated daily model. The most needed improvement may be to develop a way to determine the frequency of temperature or radiation control on photosynthesis for sunlit and shaded leaves separately in daily steps under variable weather conditions.

To further validate the daily model for applications to boreal landscape of various cover types, we also simulated a data set obtained from an aspen site. Fig. 9 shows a summary of the modeling results for this site. Again, the big-leaf model has the same problem, but the results for the daily-integrated model are better than that for the black spruce site shown in Fig. 8 in terms of the scatter and slope. The scatter is reduced because of the better spatial representativeness of the eddy-covariance technique used for measuring fluxes from the understory and soil. However, the model is still not able to simulate the days with large NPP values for the same reason as discussed for Fig. 8.

5. Conclusions

With the unprecedented simultaneous CO_2 flux measurements above and below forest canopies, we are able for the first time to examine various canopy photosynthesis models at daily steps. Big-leaf canopy photosynthesis models are the simplest and are shown to be capable of simulating the seasonal photosynthesis trends. However, we found such models greatly dampen day-to-day

variations in canopy photosynthesis simulations when compared with the measurements. Big-leaf photosynthesis models disrupted the harmony of the original leaf-level photosynthesis model through the replacement of stomatal conductance with canopy conductance. They do not adequately represent the flow of CO_2 in plant canopies because stomatal conductance is only part of the control of CO_2 flow from the free air to the photosynthetic apparatus inside leaf cells. Sunlit–shaded leaf separation is an improvement over big-leaf models, but models of this type can be in error in daily step calculations if the diurnal variability is ignored. Non-linear response of leaf photosynthesis to meteorological variables makes it inaccurate to use daily mean meteorological inputs to calculate the daily total photosynthesis without considering the diurnal variabilities. The first-order effects of the diurnal variabilities are considered in this study by performing a simplified analytical temporal integration of the Farquhar's model under the assumption of a sinusoidal radiation variation pattern. A new daily canopy photosynthesis model is therefore derived and validated with experimental data. This model captures the effects of diurnal variabilities on photosynthesis and is efficient for computation, and therefore is suitable for remote sensing applications.

Acknowledgements

We thank Dr T.A. Black of University of British Columbia for the permission to use the data from the aspen site for model validation. The senior author is indebted to Dr J. Norman of University of Wisconsin at Madison and Dr J. Berry of Stanford University for useful discussions concerning the importance of shaded leaves in boreal photosynthesis. We are grateful to Michael Sarich for his assistance in data processing.

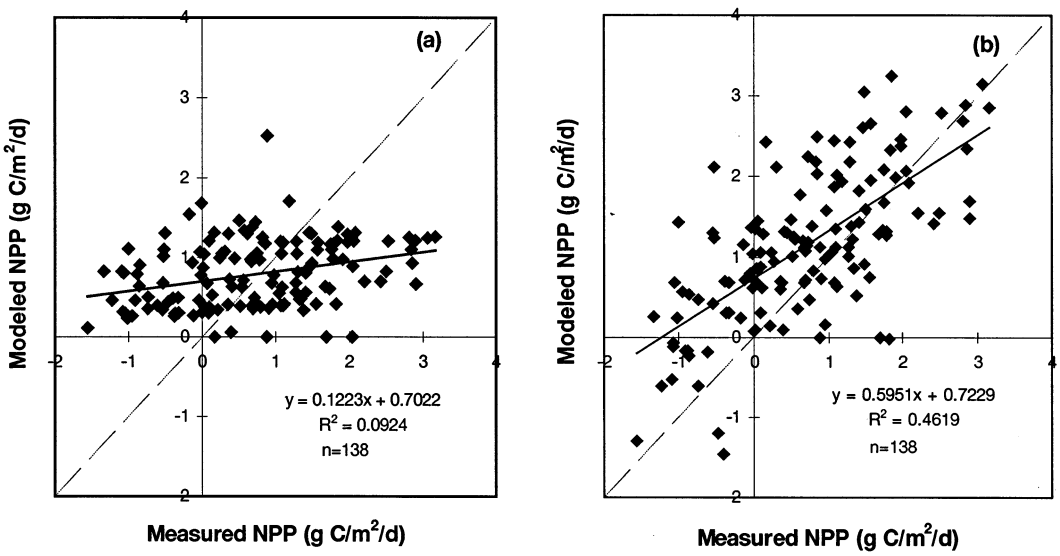

Fig. 8. One-to-one comparison of the measured NPP with the modeled NPP for a mature black spruce stand. (a) big-leaf model, and (b) daily integrated model with sunlit–shaded leaf separation.

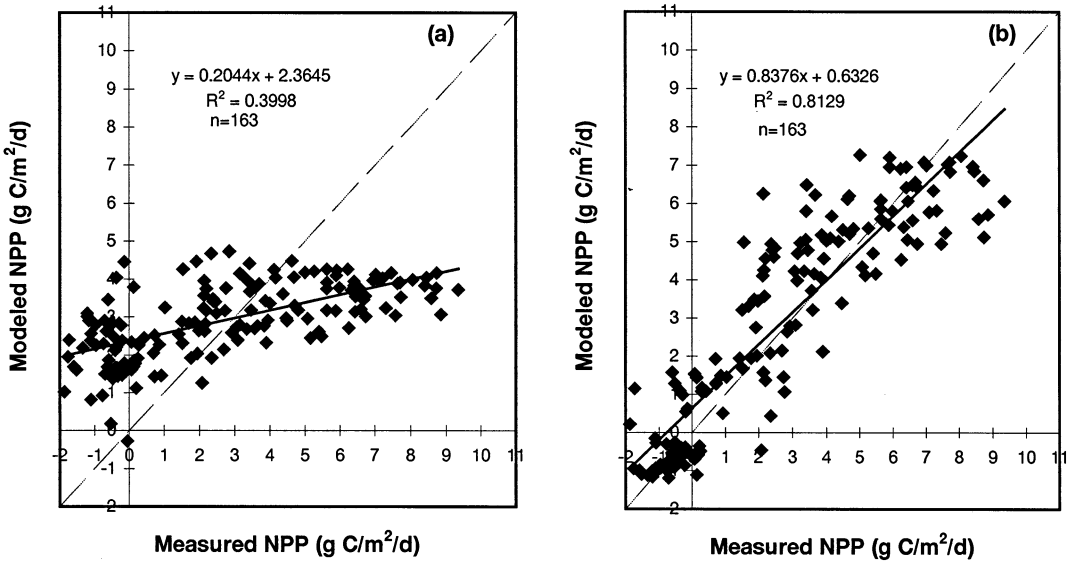

Fig. 9. One-to-one comparison of the measured NPP with the modeled NPP for a mature aspen stand. (a) big-leaf model, and (b) daily integrated model with sunlit–shaded leaf separation.

References

Aber, J.D., Reich, P.B., Goulden, M.L., 1996. Extrapolating leaf CO_2 exchange to the canopy: a generalized model of forest photosynthesis compared with measurements by eddy correlation. Oecologia 106, 257–265.

Baldocchi, D.D., 1993. Scaling water vapor and carbon dioxide exchange from leaves to a canopy: rules and tools. In: Ehleringer, J.R., Field, C.B. (Eds.), Scaling Physiological Processes: Leaf to Globe. Academic, San Diego, pp. 77–114.

Ball, J.T., 1988. An analysis of stomatal conductance. PhD thesis, Standford University, 89pp.

Black, T.A., den Hartog, G., Neumann, H.H., Blanken, P.D., Yang, P.C., Russell, C., Nesic, Z., Lee, X., Chen, S.G., Staebler, R., Novak, M.D., 1996. Annual cycle of water vapour and carbon dioxide fluxes in and above a boreal aspen forest. Global Change Biol. 2, 101–111.

Black, T.A., Chen, J.M., Lee, X., Sagar, R.M., 1991. Characteristics of shortwave and longwave irradiances under a Douglas-fir forest stand. Can. J. Forest Res. 12, 1020–1028.

Bonan, G.B., 1995. Land–atmosphere CO_2 exchange simulated by a land surface process model coupled to an atmospheric general circulation model. J. Geophys. Res. 100, 2817–2831.

Bonan, G.B., Pollard, D., Thompson, S.L., 1993. Influence of subgrid-scale heterogeneity in leaf area index, stomatal resistance, and soil moisture on grid-scale land–atmosphere interactions. J. Climate 6, 1882–1897.

Chen, J.M., 1996a. Optically-based methods for measuring seasonal variation of leaf area index in boreal conifer stands. Agric. Forest Meteorol. 80, 135–163.

Chen, J.M., 1996b. Canopy architecture and remote sensing of the fraction of photosynthetically active radiation in boreal conifer stands. IEEE Trans. Geosci. Remote Sensing 34, 1353–1368.

Chen, J.M., Rich, P.M., Gower, S.T., Norman, J.M., Plummer, S., 1997. Leaf area index of boreal forests: theory, techniques, and measurements. J. Geophys. Res. 102 (29), 429–443.

Collatz, G.J., Ball, J.T., Crivet, C., Berry, J.A., 1991. Physiological and environmental regulation of stomatal conductance, photosynthesis and transpiration: a model that includes a laminar boundary layer. Agric. Forest Meteorol. 54, 107–136.

Dang, Q.L., Margolis, H.A., Coyea, M.R., Sy, M., Collatz, G.J., 1997. Regulation of branch-level gas exchange of boreal trees: roles of shoot water potential and vapour pressure difference. Tree Physiol. 17, 521–535.

Dang, Q.L., H.A. Margolis, M., Collatz, G.J., 1998. Parameterization and testing of a coupled photosynthesis–stomatal conductance model for boreal trees. Tree Physiol. 18, 141–153.

De Pury, D.G.G., Farquhar, G.D., 1997. Simple scaling of photosynthesis from leaves to canopies without the errors of big-leaf models. Plant Cell Environ. 20, 537–557.

Denning, S.A., Collatz, G.J., Zhang, C., Randall, D.A., Berry, J.A., Sellers, P.J., Colello, G.D., Dazlich, D.A., 1996. Simulation of terrestrial carbon metabolism and atmospheric CO_2 in a general circulation model Part 1: surface carbon fluxes. Tellus 48B, 521–542.

Erbs, D.G., Klein, S.A., Duffie, J.A., 1982. Estimation of diffuse radiation fraction for hourly, daily and monthly-average global radiation. Solar Energy 28, 293–304.

Farquhar, G.D., von Caemmerer, S., Berry, J.A., 1980. A biochemical model of photosynthetic CO_2 assimilation in leaves of C_3 species. Planta 149, 78–90.

Farquhar, G.D., von Caemmerer, S., 1982. Modelling of photosynthetic response to environmental conditions. In: Lange, O.L., Nobel, P.S., Osmond, C.B., Ziegler, H. Jr (Eds.), Encyclopedia of Plant Physiology, New Series: Physiological Plant Ecology II, vol. 12B. Spring Verlag, Berlin, pp. 549–587.

Foley, J.A., 1994. Net primary productivity in the terrestrial biosphere: The application of a global model. J. Geophys. Res. 99, 20773–20783.

Foley, J.A., Prentice, I.C., Ramankutty, N., Levis, S., Pollard, D., Sitch, S., Haxeltine, A., 1996. An integrated biosphere model of land surface processes, terrestrial carbon balance and vegetation dynamics. Global Biogeochem. Cycles 10, 603–628.

Goulden, M.L., Crill, P.M., 1997. Automated measurement of CO_2 exchange at the moss surface of a black spruce forest. Tree Physiol. 17, 537–542.

Goulden, M.L., Daube, B.C., Fan, S.-M., Sutton, D.J., Bazzaz, A., Munger, J.W., Wofsy, S.C., 1997. Physiological responses of a black spruce forest to weather. J. Geophys. Res. 102 (28), 987–996.

Gower, S.T., Vogel, J.G., Norman, J.M., Kucharik, C.J., Steele, S.J., Stow, T.K., 1977. Carbon distribution and aboveground net primary productivity in aspen, jack pine, and black spruce stands in Saskatchewan and Manitoba, Canada. J. Geophys. Res. 102, 29029–29041.

Hall, F.G., Huemmrich, K.F., Goetz, S.J., Sellers, P.J., Nickeson, J.E., 1992. Satellite remote sensing of surface energy balance: success, failures, and unresolved issue in FIFE. J. Geophys. Res. 97 (19), 061–089.

Hanson, J.D., 1991. Analytical solution of the rectangular hyperbola for estimating daily net photosynthesis. Ecol. Model. 58, 209–216.

Haxeltine, A., Prentice, I.C., 1996. A general model for the light-use efficiency of primary production. Functional Ecol. 10, 551–561.

Hunt, E.R. Jr, Running, S.W., 1992. Simulated dry matter yields for aspen and spruce stand in the North American Boreal Forest. Can. J. Remote Sensing 18, 126–133.

Jarvis, P.G., Morison, J.I.L., 1981. Stomatal control of transpiration and photosynthesis. In: Jarvis, P.G., Mansfield, T.A. III (Eds.), Stomatal Physiology. Cambridge University Press, New York, pp. 247–279.

Kim, J., Verma, S.B., 1991. Modeling canopy photosynthesis: scaling up from a leaf to canopy in a temperate grassland. Agric. Forest Meteorol. 57, 187–208.

Kimball, J.S., Thornton, P.E., White, M.A., Running, S.W., 1997. Simulating forest productivity and surface-atmosphere carbon exchange in the BOREAS study region. Tree Physiol. 17, 589–599.

Leuning, R., 1990. Modelling stomatal behaviour and photosynthesis of *Eucalyptus grandis*. Aust. J. Plant. Physiol. 17, 159–175.

Liu, D.L., 1996. Incorporating diurnal light variation and canopy light attenuation into analytical equations for calculating daily gross. Ecol. Model. 93, 175–189.

Liu, J., Chen, J.M., Cihlar, J., Park, W.M., 1997. A process-based boreal ecosystem productivity simulator using remote sensing inputs. Remote Sensing Environ. 62, 158–175.

Melillo, J.M., McGuire, A.D., Kicklinghter, D.W., Moore, B. III, Vorosmarty, C.J., Schloss, A.L., 1993. Global climate change and terrestrial net primary production. Nature 363, 234–240.

Melillo, J.M., Prentice, I.C., Farquhar, G.D., Schulze, E.D., Sala, O.E., 1996. Terrestrial biotic response to environmental change and feedbacks to climate. In: Houghton, J.T., Meira Filho, L.G., Callander, B.A, Harris, N., Kattenberg, A., Maskell, K. (Eds.), Climate Change 1995. Cambridge University Press, Cambridge, pp. 445–482.

Monteith, J.L., Unsworth, M.H., 1990. Principles of Environmental Physics, 2nd ed. Edward Arnold, London.

Norman, J.M., 1982. Simulation of microclimates. In: Hatfield, J.L., Thomason, I.J. (Eds.), Biometeorology in Integrated Pest Management. Academic Press, New York, pp. 65–99.

Norman, J.M., 1993. Scaling processed between leaf and canopy levels. In: Ehleringer, J.R., Field, C.B. (Eds.), Scaling Physiological Processes: Leaf to Globe. Academic Press, San Diego, pp. 41–76.

Oke, T.R., 1990. Boundary Layer Climates, 2nd ed. Routledge, London.

Pielke, R.A., Dalu, G.A., Snook, J.S., Lee, T.J., Kittel, T.G.F., 1991. Nonlinear influence of mesoscale land use on weather and climate. J. Climate 4, 1053–1069.

Ruimy, A., Dedieu, G., Saugier, B., 1996. TURC: a diagnostic model of continental gross primary productivity and net primary productivity. Global Biogeochem. Cycle 10, 269–285.

Running, S.W., Coughlan, J.C., 1988. A general model of forest ecosystem processes for regional applications I. Hydrological balance, canopy gas exchange and primary production processes. Ecol. Model. 42, 125–154.

Running, S.W., Nemani, R.R., Peterson, D.L., Band, L.E., Potts, D.F., Pierce, L.L., Spanner, M.A., 1989. Mapping regional forest evapotranspiration and photosynthesis by coupling satellite data with ecosystem simulation. Ecology 70, 1090–1101.

Ryan, M.G., 1991. A simple method for estimating gross carbon budgets for vegetation in forest ecosystems. Tree Physiol. 9, 255–266.

Ryan, M., Lavigne, M.B., Gower, S.T., 1997. Annual carbon cost of autotrophic respiration in boreal forest ecosystems in relation to species and climate. J. Geophys. Res. 102, 28871–28883.

Sands, P.J., 1995. Modelling canopy production. II. From single-leaf photosynthetic parameters to daily canopy photosynthesis. Aust. J. Plant. Physiol. 22, 603–614.

Sellers, P.J., Berry, J.A., Collatz, G.J., Field, C.B., Hall, F.G., 1992. Canopy reflectance, photosynthesis, and transpiration. III. A reanalysis using improved leaf models and a new canopy integration scheme. Remote Sensing Environ. 42, 187–216.

Sellers, P.J., Randall, D.A., Collatz, G.J., Berry, J.A., Field, C.B., Dazlich, D.A., Zhang, C., Collelo, G.D., Bounoua, L., 1996. A revised land surface parameterization (SiB2) for atmospheric GCMs. Part I: model formulation. J. Climate 9, 676–705.

Sellers, P., Hall, F.G., Kelly, R.D., Black, A., Baldocchi, D., Berry, J., Ryan, M., Ranson, K.J., Crill, P.M., Lettenmaier, D.P., Margolis, H., Cihlar, J., Newcomer, J., Fitzjarrald, D., Jarvis, P.G., Gower, S.T., Halliwell, D., Williams, D., Goodison, B., Wichland, D.E., Guertin, F.E., 1997. BOREAS in 1997: scientific results, overview and future directions. J. Geophys. Res. 102, 28731–28769.

Steele, S.J., Gower, S.T., Vogel, J.G., Norman, J.M., 1997. Root mass, net primary production and turnover in aspen, jack pine and black spruce forests in Saskatchewan and Manitoba, Canada. Tree Physiol. 17, 577–587.

Trost, N., 1990. An approximate formula for the daily photoproduction of forest tree canopies. Ecol. Model. 49, 297–309.

Wang, Y.-P., Leuning, R., 1998. A two-leaf model for canopy conductance, photosynthesis and partitioning of available energy. I: model description and comparison with a multilayered model. Agric. Forest Meteorol. 91, 89–111.

Wood, E.F., Lakshmi, V., 1993. Scaling water and energy fluxes in climate system: three land-atmospheric modeling experiments. J. Climate 6, 839–857.

Woodward, F.I., Smith, T.M., Emanuel, W.R., 1995. A global land primary productivity and phytogeography model. Global Biogeochem. Cycle 9, 471–490.

Wullschleger, S.D., 1993. Biochemical limitations to carbon assimilation in C_3 plants — a retrospective analysis of the A/C_i curves from 109 species. J. Exp. Botany 44, 907–920.